AGU PUBLICATIONS

Geophysical Research Letters

RESEARCH LETTER
10.1002/2016GL071700

Key Points:
- The observed discrepancy between laboratory- and field-based stress drop estimates can be linked to fault roughness and strength asperities
- Field-based estimates are biased low, not considering fault roughness. Lab-based estimates are biased high, representing "only" asperities
- Smooth faults require lower stress drops than rough ones to generate the same-size earthquake, suggesting that the prior are, respectively, weaker

Supporting Information:
- Supporting Information S1
- Data Set S1
- Data Set S2
- Data Set S3
- Data Set S4
- Data Set S5
- Data Set S6
- Data Set S7
- Data Set S8
- Data Set S9
- Data Set S10
- Data Set S11
- Data Set S12

Correspondence to:
O. Zielke,
olaf.zielke@kaust.edu.sa

Citation:
Zielke, O., M. Galis, and P. M. Mai (2017), Fault roughness and strength heterogeneity control earthquake size and stress drop, *Geophys. Res. Lett.*, *44*, 777–783, doi:10.1002/2016GL071700.

Received 23 OCT 2016
Accepted 10 JAN 2017
Accepted article online 13 JAN 2017
Published online 26 JAN 2017

Fault roughness and strength heterogeneity control earthquake size and stress drop

O. Zielke[1], M. Galis[1], and P. M. Mai[1]

[1]Department of Earth Science and Engineering, King Abdullah University of Science and Technology, Thuwal, Saudi Arabia

Abstract An earthquake's stress drop is related to the frictional breakdown during sliding and constitutes a fundamental quantity of the rupture process. High-speed laboratory friction experiments that emulate the rupture process imply stress drop values that greatly exceed those commonly reported for natural earthquakes. We hypothesize that this stress drop discrepancy is due to fault-surface roughness and strength heterogeneity: an earthquake's moment release and its recurrence probability depend not only on stress drop and rupture dimension but also on the geometric roughness of the ruptured fault and the location of failing strength asperities along it. Using large-scale numerical simulations for earthquake ruptures under varying roughness and strength conditions, we verify our hypothesis, showing that smoother faults may generate larger earthquakes than rougher faults under identical tectonic loading conditions. We further discuss the potential impact of fault roughness on earthquake recurrence probability. This finding provides important information, also for seismic hazard analysis.

1. Background and Motivation

Earthquakes can be regarded as frictional phenomena that release tectonically or otherwise accumulated stresses in the form of slip along generally preexisting fault surfaces [e.g., *Scholz*, 2002; *Aki and Richards*, 2009]. The coseismically released static stress drop $\Delta\tau$—defined as the average change in shear stress on a rupture surface before and after a slip event—is a fundamental quantity of the rupture process, bearing information on an earthquake's frictional breakdown during sliding, its seismic energy release, the frequency content of radiated seismic waves, and earthquake recurrence probability [e.g., *Reid*, 1910; *Brune*, 1970; *Scholz*, 2002; *Aki and Richards*, 2009]. Static stress drop is relevant for hazard assessment and the general understanding of earthquake physics. Estimates of $\Delta\tau$ based on seismological observations employ a simplified representation of the earthquake source that correlates fault slip, moment release, or frequency content of radiated seismic waves to stress drop [e.g., *Brune*, 1970; *Kanamori and Anderson*, 1975; *Hanks*, 1977; *Aki and Richards*, 2009; *Allmann and Shearer*, 2009]. The corresponding values of $\Delta\tau$ are centered at ~3–4 MPa and do not change systematically with earthquake size, which is taken as evidence for self-similar earthquake scaling [e.g., *Kanamori and Anderson*, 1975; *Hanks*, 1977; *Allmann and Shearer*, 2009]. On the other hand, laboratory friction experiments indicate an almost complete breakdown in frictional resistance during sliding when coseismic slip velocities are reached [e.g., *Han et al.*, 2007; *Di Toro et al.*, 2011]. The observed large change in friction (typically $\Delta\mu \geq 0.5$) in such experiments, combined with effective normal stresses at seismogenic depths (σ_{eff}), yields coseismic stress drops $\Delta\tau = \Delta\mu\sigma_{\text{eff}}$ that exceed those derived from seismological observations by multiples of 10. Consequently, laboratory- and field-based estimates of coseismic stress drop $\Delta\tau$ are incompatible, questioning the validity of current $\Delta\tau$ estimates and the conclusions that are based on them.

We conjecture that the strong discrepancy in $\Delta\tau$ estimates is due to the nonplanarity of natural rupture surfaces [e.g., *Power et al.*, 1988; *Sagy et al.*, 2007; *Candela et al.*, 2012; *Brodsky et al.*, 2016], the spatial heterogeneity of rock strength on the fault (here strength refers to a fault's potential to sustain some amount of shear stress before slippage occurs [e.g., *Ripperger and Mai*, 2004; *Konca et al.*, 2008; *Mai and Thingbaijam*, 2014]), and their combined effect on an earthquake's slip distribution and moment release. We employ large-scale numerical simulations to investigate how the surface roughness of a fault and its strength heterogeneity affect average slip $\overline{D}$ and seismic moment M_0 that are associated to stress drop $\Delta\tau$. After describing the numerical model that was used in this study, we present our results and conclusion. The online supporting information contains additional data on model formulation and adopted physical parameters.

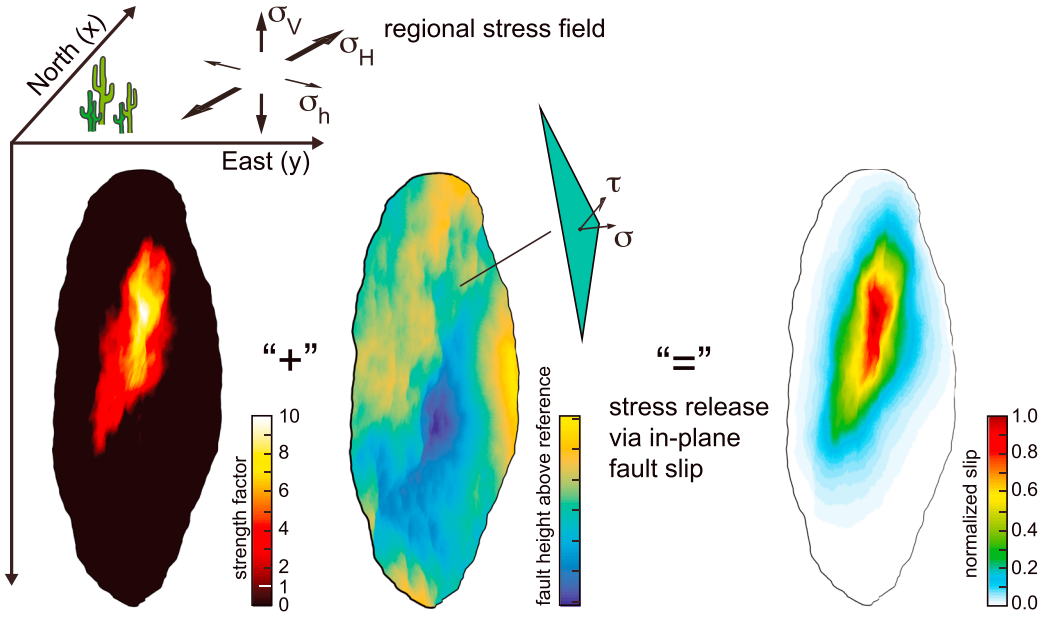

Figure 1. Overview of our computational setup. We consider a circular rupture surface that is subdivided into triangular fault patches. (left) We assign a strength factor to each triangular fault patch, indicating the patch's potential to sustain some amount of stress before slippage. We investigate homogeneous (not shown) and heterogeneous strength distributions. The latter are modeled as a self-similar 2-D random field while further employing a minimum-strength cutoff level (see online supporting information). Those strength distributions are normalized to provide on-fault unit strength. (middle) Fault geometric roughness is also modeled as a self-similar 2-D random field and quantified through dimensionless roughness metric σ_{RMS} (see online supporting information). We resolve a regional stress field (defined by principal stresses σ_H, σ_h, and σ_V) onto the triangular fault patches according to their orientation within that stress field (providing normal and shear traction σ and τ acting on the fault patch) and their assigned strength factor. (right) The applied shear stresses are then released via fault slip.

2. Model Formulation

We utilize a quasi-static elastic model for our analysis. As such, it does not capture the dynamic aspects of rupture propagation, and no seismic radiation occurs. With a simplified representation of the earthquake source, adopting this model is justified as it relates closely to the analytical formulations for simple crack-like rupture [*Brune*, 1970; *Kanamori and Anderson*, 1975; *Hanks*, 1977] with which we compare and normalize our results.

We define a circular fault with randomly varying diameter and divide it into approximately equal-sized triangular fault patches (Figures 1 and S1 in the supporting information). The fault is embedded in a homogeneous elastic full-space and we employ formulations by *Nikkhoo and Walter* [2015] to calculate the medium's elastic response to slip. The fault's complex geometry (i.e., fault roughness) is parameterized as a 2-D random field that follows the von Karman autocorrelation function (ACF) (see online supporting information) [*Mai and Beroza*, 2002]. We model fault roughness to be fractally self-similar (Hurst exponent $H = 1$) as opposed to self-affine ($H < 1$). While this approach may present a simplification, it still captures the main characteristics of the surface roughness of natural faults [see *Candela et al.*, 2012; *Shi and Day*, 2013]. Furthermore, adopting a self-similar roughness model enables us to provide scale-independent roughness quantification and fault representations: the modeled fault may equally well represent a circular fault with 1 m diameter as well as 10 km diameter or else. Fault roughness is then quantified via the dimensionless, single-value metric σ_{RMS} (equation (1)):

$$\sigma_{\mathrm{RMS}} = \frac{1}{L}\sqrt{\frac{1}{A}\Sigma_{i=1}^{N} h_i^2 da} \tag{1}$$

where L is 1-D fault length (here diameter), A is the fault area, i is the index of individual fault patch, N is the number of fault patches, h is the patch height above a planar reference, and da is the fault patch area [e.g., *Power et al.*, 1988].

For the method, we need to provide a spatial distribution of releasable stress drop, $\Delta\tau_i$. We start with a stress tensor representing the regional stress state (oriented for a strike-slip fault) in a tectonically active region and resolve it onto the triangular fault patches (Figures 1 and S2). Shear stress τ_i therefore varies (slightly) from patch to patch, depending on their orientation relative to the stress tensor. We further assign friction coefficients (uniform across the whole fault) to calculate the normal stress that acts on each patch assuming depth independence, $\sigma_{\text{eff},i} = \tau_i/\mu_s$ (static friction coefficient $\mu_s = 0.6$). Consistent with laboratory friction experiments, we assume a nearly complete breakdown in frictional resistance once sliding occurs (dynamic friction coefficient $\mu_d = 0.1$; $\Delta\mu = \mu_s - \mu_d = 0.5$ [e.g., *Di Toro et al.*, 2011]), defining the static stress drop as $\Delta\tau_i = \Delta\mu\ \sigma_{\text{eff},i}$. Next, we assign a strength factor k_i to each fault patch *i*. With respect to the classic friction law this strength factor modifies $\sigma_{\text{eff},i}$ (and hence $\Delta\tau_i$) acting on the fault patch, $\Delta\tau_i = \Delta\mu\ k_i\sigma_{\text{eff},i}$. In case of homogeneous strength, all parts of the fault are equally strong, and hence, $k_i = 1$ for each patch. Heterogeneous strength distributions are modeled differently. First, we generate a self-similar 2-D random field employing the von Karman ACF (see online supporting information). This field is not causally related to the fault's fractal geometry. While a distinct correlation of geometry and strength has been suggested [e.g., *Brodsky et al.*, 2016], we intentionally do not prescribe the physical cause that generates strength heterogeneity, and hence, we parameterize both fields independent from each other. Next we pick a percentile (between 0 and 80) that serves as a "strength water level" and determine the random-field value that corresponds to this percentile (k_{WL}). We then set all field values below k_{WL} equal to k_{WL}, subtract k_{WL} from the field, and then scale this field such that $k_{\text{mean}} = 1$ on the rupture surface (Figure S2). Lastly, we multiply k_i with $\sigma_{\text{eff},i}$ for each fault patch, modifying the releasable amount of shear stress $\Delta\tau_i = \Delta\mu\ k_i\sigma_{\text{eff},i}$ for each patch. As a result—depending on percentile water level value of a given model realization and the fractal characteristics of the field—$\Delta\tau_i$ may significantly exceed the fault's average stress drop $\Delta\tau$ (Figure 1). The strength factor k_i therefore acts to redistribute the fault's strength (and hence stress drop), while keeping its mean value constant.

We assume that rupture initiates simultaneously across the whole fault surface; that is, each part of the fault instantaneously releases the applied shear stress $\Delta\tau_i$ through fault slip until all of $\Delta\tau_i$ is released. Numerically, this is achieved through an iterative stress-release loop [e.g., *Tullis et al.*, 2012]: During each iteration, all fault patches release their currently applied shear stress $\Delta\tau_i$ via fault slip. This slip will modify the shear and normal stresses on all other fault patches (the change in normal stress may cause fault patches to clamp or unclamp, inhibiting or promoting further in-plane slip along them, respectively). The iterative loop is finished once $\Delta\tau_i$ on all patches is below a numerical threshold value τ_{thresh} (see online supporting information) [*Tullis et al.*, 2012], providing a slip distribution along the fault surface (Figures 1 and S4).

For each model realization (i.e., combination of randomly generated fault roughness and strength distribution), we determine average slip $\overline{D}$ and the corresponding moment release $M_0 = GA\overline{D}$, where G is the shear modulus and A is the ruptured area. We use subindex r to refer to geometrically rough faults (e.g., $\overline{D}_r$ is average slip on a rough fault) and subindex p for its planar equivalent. Rough-fault values are normalized with their planar-fault equivalents to define $\overline{D}_n = \overline{D}_r/\overline{D}_p$ and $M_{0,n} = M_{0,r}/M_{0,p}$, respectively.

3. Results

3.1. Sampling the Fractal Fault Surface

The adopted numerical setup requires a sufficiently fine spatial discretization of the rupture surface to represent its fractal characteristics [e.g., *Power et al.*, 1988; *Sagy et al.*, 2007; *Candela et al.*, 2012; *Brodsky et al.*, 2016; *Zielke and Mai*, 2016] with regards to slip $\overline{D}$ associated with stress drop $\Delta\tau$, i.e., the fault's elastic response. We identify the corresponding model resolution (patch number N) by examining the average amount of induced stress along a rupture surface due to slip along that surface (also known as back slip model [e.g., *Tullis et al.*, 2012]) for varying spatial discretization. We find that the corresponding metric $\Delta\overline{\tau}_{\text{norm}}/\Delta N$ (see online supporting information) asymptotically converges to zero (Figure 2a), indicating that a parameterization with ~10^5 fault patches suffices to approximate a fractal rupture surface with respect to the fault's elastic response. The identified parameterization may have a profound physical meaning, defining an effective inner length scale for earthquake rupture: roughness expressions smaller than this length scale only marginally affect the fault's elastic response and may be omitted, while

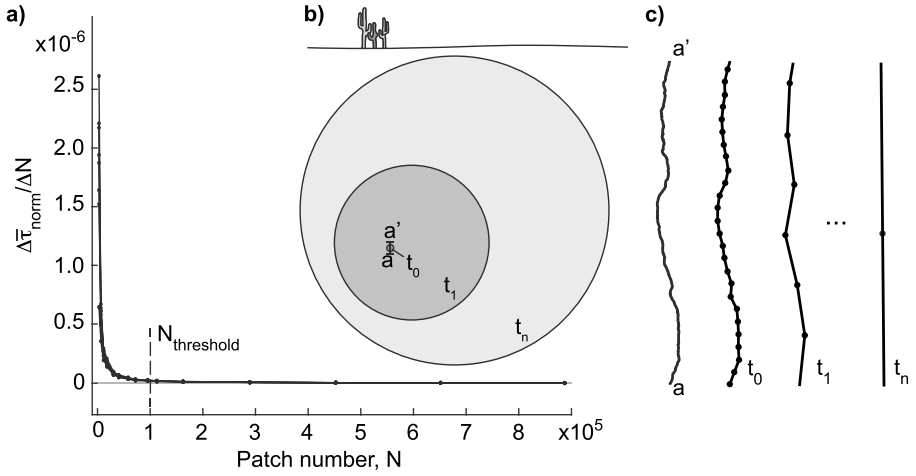

Figure 2. (a) Approximation of eight randomly generated fractal fault surfaces with different model resolutions. $\Delta\bar{\tau}_{norm}/\Delta N$ converges toward zero for $N > 10^5$ patches. (b) Idealized growth of a rupture surface through time t and the location of a cross-sectional roughness profile $a - a'$ on the initiation area. (c) Fault roughness along $a - a'$ exhibits self-similarity. At rupture initiation t_0, only roughness features larger than the inner length scale effectively influence propagation (indicated by the profile resolution at t_0). Smaller roughness features may be omitted with regards to the slip-stress relationship. As the rupture grows from t_0 to t_1 and t_n, the inner length scale increases in absolute terms (as it is defined relative to rupture area). The growing rupture becomes increasingly insensitive to small-scale fault roughness.

roughness expressions larger than this length scale need to be considered to properly incorporate the fractal character of fault roughness. Because this inner length scale is defined relative to rupture area, it increases in absolute terms as the rupture area itself grows (Figures 2b and 2c). For instance, roughness expressions at centimeter scale may distinctly influence rupture evolution for source dimensions in the meter-scale range but will have a negligible effect once the corresponding rupture area expands to the kilometer scale. Following the logic of this example, we infer that the concept of an inner length scale also extends to self-affine fault roughness. Further note that the concept of an inner length scale is defined for a crack-like rupture. We speculate that pulse-like ruptures will exhibit a similar length scale that may be related to the pulse width, rather than rupture area.

3.2. Homogenous Fault Strength

To understand the relationship between σ_{RMS} and $M_{0,n}$, we first discuss rough faults with spatially homogeneous strength on the rupture surface. The corresponding, essentially identical relationship between σ_{RMS} and $\overline{D}_n$ may be found in Figure S5. Figure 3 shows that $M_{0,n}$ is substantially modified by the presence of fault roughness and exhibits an inverse relationship with it. Rough faults (with higher σ_{RMS} values) generate less seismic moment per stress drop $\Delta\tau$, relative to what is predicted for a planar fault [e.g., *Kanamori and Anderson*, 1975; *Aki and Richards*, 2009]. For instance, a rough fault with σ_{RMS} ~0.01 —a typical value for natural faults [e.g., *Power et al.*, 1988; *Sagy et al.*, 2007; *Candela et al.*, 2012; *Brodsky et al.*, 2016]—generates approximately half of the seismic moment than a planar fault, for the same stress drop (Figure 3). Formulated differently, a rough fault with σ_{RMS} ~0.01 requires an approximately 2 times larger stress drop to generate the same seismic moment as the planar fault. This finding suggests that current stress drop estimates for natural earthquakes may be biased low because they do not account for the effect of fault roughness.

The observed dependency of $M_{0,n}$ on σ_{RMS} is empirically well described by the function (equation (2)) obtained through least squares regression (Figure 3).

$$\gamma(\sigma_{RMS}) = \frac{0.0021\sigma_{RMS} + 0.0001}{\sigma_{RMS}^2 + 0.0021\sigma_{RMS} + 0.0001} \quad (2)$$

This function allows incorporating the effect of fault roughness into earthquake-scaling relations [e.g., *Kanamori and Anderson*, 1975; *Aki and Richards*, 2009] that correlate stress drop to slip or seismic moment

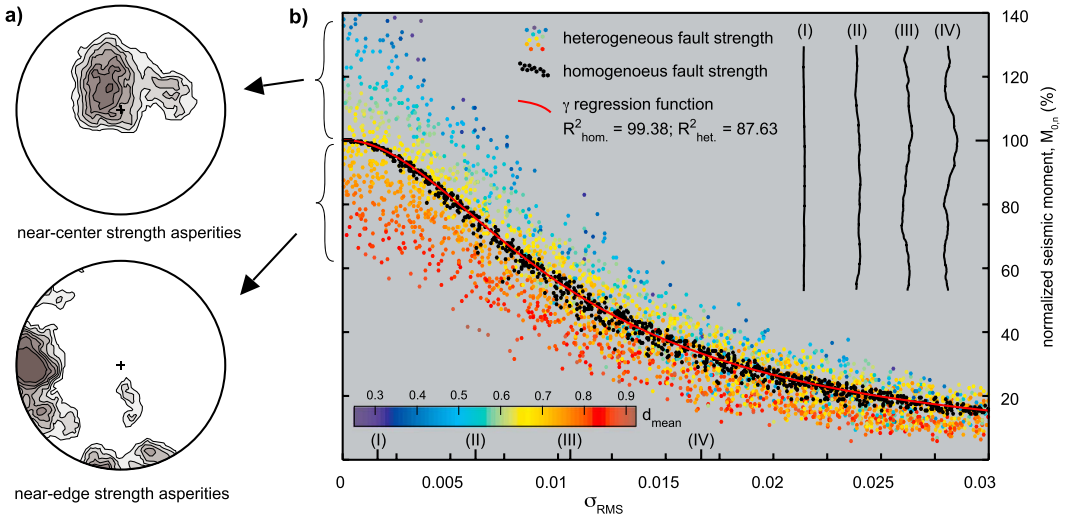

Figure 3. Relationship between normalized seismic moment $M_{0,n}$ and σ_{RMS}. (a) Two exemplary fault surfaces with spatially heterogeneous strength distribution and their respective contribution to the $M_{0,n} - \sigma_{RMS}$ relationship. Ruptures with near-center strength asperities increase $M_{0,n}$ relative to the homogeneous strength case. Near-edge strength asperities have the opposite effect. (b) Relationship between fault roughness metric σ_{RMS} and normalized seismic moment $M_{0,n}$ for homogeneous (in black) and heterogeneous strength distributions. The latter are color coded by strength-weighted average distance between asperities and the center of the circular fault surface d_{mean}. In both cases, we observe an inverse relationship between σ_{RMS} and $M_{0,n}$: rough faults release less seismic moment per tectonic loading than smooth ones. Least squares regression of the respective point clouds with a rational function provides an excellent representation of the data (indicated by the R^2 values). On-fault roughness profiles (I to IV) for four exemplary roughness values are presented for visual guidance on the meaning of respective σ_{RMS} values.

by substituting $\overline{D}$ with $\overline{D}_r = \gamma\overline{D}_p$ and M_0 with $M_{0,r} = \gamma\, M_{0,p}$. For circular crack-like ruptures with radius R and shear modulus G, this leads to

$$\Delta\tau = \frac{7\pi}{16} G{\cdot}\gamma\frac{\overline{D}_p}{R} \tag{3}$$

$$\Delta\tau = \frac{7}{16}{\cdot}\gamma\frac{M_{0,p}}{R^3} \tag{4}$$

Moreover, in the conceptual framework of fault friction we find that $\overline{D}$ (i.e., $\gamma\overline{D}_p$) is proportional to $\Delta\mu$. The observed decrease in average slip per stress drop due to fault roughness corresponds to a decreased frictional breakdown during sliding and thus a decrease in $\Delta\mu$. Hence, fault roughness may be regarded as a bulk frictional agent [*Griffith et al.*, 2010; *Fang and Dunham*, 2013], modifying the change in frictional resistance that is associated with a given stress drop (equation (5)).

$$\Delta\mu_r = \gamma{\cdot}\Delta\mu = \frac{\Delta\tau}{\sigma_{\text{eff}}} \tag{5}$$

If fault roughness and geometric complexity of fault networks evolve over geologic times [e.g., *Wesnousky*, 1988; *Brodsky et al.*, 2011], then structurally mature (smoother) faults might generate larger earthquakes per stress drop $\Delta\tau$ than their less mature (rougher) and geometrically more complex counterparts (Figure 3). Further, considering that roughness is a controlling factor for fault strength [*Brodsky et al.*, 2016]—and doing so in light of the stress renewal concept [e.g., *Reid*, 1910; *Scholz*, 2002; *Aki and Richards*, 2009]—implies that an earthquake's recurrence probability may be affected by fault roughness. Therefore, smoother (more mature) faults are weaker than rough (immature) ones [*Brodsky et al.*, 2016], the earthquakes on smooth faults exhibit smaller stress drops, and smooth faults are faster to regain the coseismically released stresses.

3.3. Heterogenous Fault Strength

So far, we considered spatially homogeneous on-fault strength distributions. Natural faults and the earthquakes occurring on them are affected also by heterogeneous strength over the rupture surface them [e.g., *Somerville et al.*, 1999; *Mai and Beroza*, 2002; *Ripperger and Mai*, 2004; *Kanamori and Brodsky*, 2004;

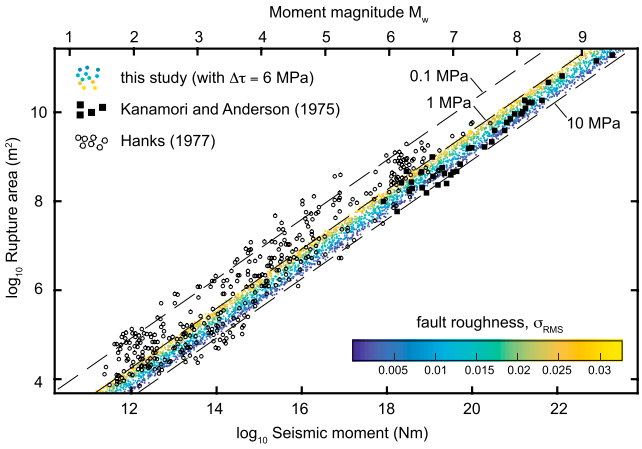

Figure 4. Relationship between seismic moment release and corresponding rupture area for natural earthquakes (solid black dots and squares) and our simulation results (color coded by roughness of the ruptured surface). For reference, the dashed lines indicate the stress drops for crack-like rupture along planar rupture surfaces. Using a stress drop of 6 MPa on geometrically rough rupture surfaces, along with the spatial heterogeneity of fault strength, explains the observational data in the 1–10 MPa, planar-reference range. Stress drop is not required to vary as much as previously suggested if fault geometry and strength heterogeneity are accounted for.

Konca et al., 2008; *Mai and Thingbaijam*, 2014]—including asperities that constitute the majority of a fault's strength and nonasperities that contribute little to strength (Figure 1). The strength and corresponding stress drop of an asperity may greatly exceed the respective mean values for the whole rupture surface—depending on asperity size relative to rupture area of the earthquake [e.g., *Somerville et al.*, 1999; *Mai and Beroza*, 2002; *Ripperger and Mai*, 2004; *Kanamori and Brodsky*, 2004; *Konca et al.*, 2008; *Mai and Thingbaijam*, 2014]. Indeed, the inferred coseismic stress drops on those asperities [e.g., *Ripperger and Mai*, 2004; *Mai and Thingbaijam*, 2014] compare well with stress drops suggested by high-speed laboratory friction experiments [e.g., *Kanamori and Brodsky*, 2004; *Han et al.*, 2007; *Di Toro et al.*, 2011]. We conclude that laboratory friction experiments portray "only" the rupture behavior of strength asperities. In contrast, natural earthquakes rupture both strength asperities and nonasperities, so that the corresponding stress drop estimates represent a spatially averaged rupture behavior. The discrepancy between field-based and laboratory-based estimates of $\Delta\tau$ is primarily related to the presence of fault strength heterogeneity. In the present study we introduce this heterogeneity by modifying $\sigma_{\mathrm{eff},i}$ via the strength factor k_i. Other physical parameters and processes may have a similar effect [*Parsons and* Minasian, 2015].

Our simulations show that model realizations with spatially heterogeneous strength exhibit the same general dependency of $\overline{D}_n$ and $M_{0,n}$ on σ_{RMS} as the homogeneous strength cases, however, with larger absolute variability that inversely depends on σ_{RMS} (Figures 3 and S5). This variability remains constant relative to the expected value of γ and is well described by a Gaussian probability distribution with zero mean and standard deviation = 0.2 γ (Figure S6). Next, we investigate the strength-weighted average distance d_{mean} (see online supporting information) between asperity location and the center of the circular fault surface (color coding in Figures 3 and S5 for heterogeneous-strength simulations). We observe an inverse relationship between d_{mean} and $M_{0,n}$: ruptures with near-center strength asperities (small d_{mean}) are associated with a larger moment release, compared to ruptures that have near-edge strength asperities (Figure 3). This observation relates to an edge effect that partially confines rupture growth to the asperity area due to its proximity to a fault boundary, thus lowering the overall rupture area and associated slip amount (Figure S7). Therefore, the on-fault positions of strength asperities are the controlling factor for an earthquake's moment release.

4. Conclusion

Figure 3 indicates that an earthquake's moment release may vary widely depending on the geometric roughness of the rupture surface and the location of strength asperities (e.g., $M_{0,n}$ between 10 and 140% for σ_{RMS} between 0 and 0.03). Without considering fault roughness and strength heterogeneity, this variability in moment release would be attributed to stress drop variations (Figure 4). However, we show that the reported range of stress drop estimates for natural earthquakes [e.g., *Kanamori and Anderson*, 1975; *Hanks*, 1977; *Allmann and Shearer*, 2009] can be produced with a single stress drop value, generating variable slip and moment release on rough faults with different roughness metrics and strength asperity locations (Figure 4). The actual variability in fault-averaged stress drop may therefore be smaller than what is currently assumed, which in turn relates to types and effectiveness of weakening mechanisms that operate during the rupture process.

Small- to moderate-sized earthquakes may exhibit an apparently smaller stress drop than predicted by our numerical simulations (Figure 4). We point out that we modeled strength asperities to reproduce characteristics observed in laboratory friction experiments—with a nearly complete breakdown in frictional resistance. It is plausible that not all ruptures (particularly smaller-sized ones) are capable of reaching the conditions to initiate the weakening mechanisms that cause this extreme frictional decay [e.g., *Kanamori and Brodsky*, 2004; *Han et al*., 2007; *Di Toro et al*., 2011]. Those earthquakes would exhibit a lower stress drop on strength asperities and consequently over the entire rupture surface. It is also plausible that the rupture surfaces on which those small- to moderate-sized events occur are even rougher ($\sigma_{RMS} > 0.03$) than what we captured in our simulations (Figure 4).

Our study shows that geometric fault roughness and on-fault strength heterogeneity strongly affect an earthquake's seismic moment release. Here we only considered a fully elastic medium. Presence of off-fault damage, an efficient energy sink, is likely further increasing the amount of stress required to generate a certain earthquake size. It is important to further investigate how these parameters influence earthquake rupture characteristics (e.g., earthquake recurrence probability). Fault roughness and strength heterogeneity can also be incorporated into existing (scaling) relationships to provide a more comprehensive framework to study and understand the earthquake rupture process.

Acknowledgments
The research reported in this publication was supported by funding from King Abdullah University of Science and Technology (KAUST). Numerical simulations for this study were carried out on the SHAHEEN II supercomputer at KAUST. Figures in the main manuscript and the online supporting information provide all the data used in this investigation. Raw data (of on-fault slip distributions) and computer codes used in this study are available from the corresponding author upon reasonable request. No financial or other types of conflicts of interest exist for the authors regarding this manuscript. We want to thank the Editor and reviewers for their construction criticism and helpful comments that improved this study.

References

Aki, K., and P. G. Richards (2009), *Quantitative Seismology*, Univ. Science Books, Suasalito, Calif.
Allmann, B. A., and P. M. Shearer (2009), Global variations of stress drop for moderate to large earthquakes, *J. Geophys. Res.*, *114*, B01310, doi:10.1029/2008JB005821.
Brodsky, E. E., J. D. Kirkpatrick, and T. Candela (2016), Constraints from fault roughness on the scale-dependent strength of rocks, *Geology*, *44*, 19–22.
Brodsky, E. E., J. J. Gilchrist, A. Sagy, and C. Collettini (2011), Faults smooth gradually as a function of slip, *Earth Planet. Sci. Lett.*, *302*, 185–193.
Brune, J. (1970), Tectonic stress and the spectra of seismic shear waves from earthquakes, *J. Geophys. Res.*, *75*, 4997–5009, doi:10.1029/JB075i026p04997.
Candela, T., F. Renard, Y. Klinger, K. Mair, J. Schmittbuhl, and E. E. Brodsky (2012), Roughness of fault surfaces over nine decades of length scales, *J. Geophys. Res.*, *117*, B08409, doi:10.1029/2011JB009041.
Di Toro, G., R. Han, T. Hirose, N. De Paola, S. Nielsen, K. Mizoguchi, F. Ferri, M. Cocco, and T. Shimamoto (2011), Fault lubrication during earthquakes, *Nature*, *471*, 494–499.
Fang, Z., and E. M. Dunham (2013), Additional shear resistance from fault roughness and stress levels on geometrical complex faults, *J. Geophys. Res. Solid Earth*, *118*, 3642–3654, doi:10.1002/jgrb.50262.
Griffith, W. A., S. Nielsen, G. DiToro and S. A. F. Smith (2010), Rough faults, distributed weakening, and off-fault deformation, *J. Geophys. Res.*, *115*, B08409, doi:10.1029/2009JB006925.
Han, R., T. Shimamoto, T. Hirose, J.-H. Ree, and J. Ando (2007), Ultralow friction of carbonate faults caused by thermal decomposition, *Science*, *316*, 878–881.
Hanks, T. (1977), Earthquake stress drops, ambient tectonic stresses and stresses that drive plate motions, *Pure Appl. Geophys.*, *115*, 441–458.
Kanamori, H., and D. L. Anderson (1975), Theoretical basis of some empirical relations in seismology, *Bull. Seismol. Soc. Am.*, *65*, 1073–1095.
Kanamori, H., and E. E. Brodsky (2004), The physics of earthquakes, *Rep. Prog. Phys.*, *67*, 1429–1496.
Konca, A. O., et al. (2008), Partial rupture of a locked patch of the Sumatra megathrust during the 2007 earthquake sequence, *Nature*, *456*, 631–635.
Mai, P. M., and G. C. Beroza (2002), A spatial random field model to characterize complexity in earthquake slip, *J. Geophys. Res.*, *107*, B112308, doi:10.1029/2001JB000588.
Mai, P. M., and K. K. S. Thingbaijam (2014), SRCMOD: An online database of finite source rupture models, *Seismol. Res. Lett.*, *85*, 1348–1357.
Nikkhoo, M., and T. R. Walter (2015), Triangular dislocation: An analytical, artifact-free solution, *Geophys. J. Int.*, *201*, 1117–1139.
Parsons, T., and D. L. Minasian (2015), Earthquake rupture process recreated from a natural fault surface, *J. Geophys. Res. Solid Earth*, *120*, 7852–7862, doi:10.1002/2015JB012448.
Power, W. L., T. E. Tullis, and J. D. Weeks (1988), Roughness and wear during brittle faulting, *J. Geophys. Res.*, *93*, 15,268–15,278, doi:10.1029/JB093iB12p15268.
Reid, H. F. (1910), The mechanics of the earthquake, the California earthquake of April 18, 1906, *Report of the State Investigation Commission, Vol.* 2 (Carnegie Institution of Washington).
Ripperger, J., and P. M. Mai (2004), Fast computation of static stress changes on 2D faults from final slip distributions, *Geophys. Res. Lett.*, *31*, L18610, doi:10.1029/2004GL020594.
Sagy, A., E. E. Brodsky, and G. J. Axen (2007), Evolution of fault-surface roughness with slip, *Geology*, *35*, 283–286.
Scholz, C. H. (2002), *The Mechanics of Earthquakes and Faulting*, Cambridge Univ. Press, Cambridge.
Shi, Z., and S. M. Day (2013), Rupture dynamics and ground motion from 3-D rough-fault simulations, *J. Geophys. Res. Solid Earth*, *118*, 1122–1141, doi:10.1002/jgrb.50094.
Somerville, P., K. Irikura, R. Graves, S. Sawada, D. Wald, N. Abrahamson, Y. Iwasaki, T. Kagawa, N. Smith, and A. Kowada (1999), Characterizing crustal earthquake slip models for the prediction of strong ground motion, *Seismol. Res. Lett.*, *70*, 59–80.
Tullis, T. E., et al. (2012), Generic earthquake simulator, *Seismol. Res. Lett.*, *83*, 959–963.
Wesnousky, S. G. (1988), Seismological and structural evolution of strike-slip faults, *Nature*, *335*, 340–343.
Zielke, O., and P. M. Mai (2016), Subpatch roughness in earthquake rupture investigations, *Geophys. Res. Lett.*, *43*, 1893–1900, doi:10.1002/2015GL067084.